

19% Efficient N-Type All-Back-Contact Silicon Wafer Solar Cells With Planar Front Surface

Ngwe Zin¹, Andrew Blakers¹, Keith McIntosh¹, Evan Franklin¹, Teng Kho¹, Johnson Wong², Thomas Mueller², Armin G. Aberle², Zhiqiang Feng³, and Qiang Huang³

¹ Australian National University, Australia

² Solar Energy Research Institute of Singapore, National University of Singapore, Singapore

³ State Key Laboratory of PV Science and Technology, Trina Solar Limited, China

ABSTRACT

19% efficient all-back-contact silicon wafer solar cells developed on n-type FZ material at the Australian National University (ANU) are reported as part of a collaboration between the PV manufacturer Trina Solar and the Solar Energy Research Institute of Singapore (SERIS). The cells, having an area of $4 \times 4 \text{ cm}^2$, incorporate a heavy phosphorus diffusion (n^+ BSF) and boron emitter (p^+) at the rear, and a light phosphorus diffusion (FSF) at the front. The boron emitter covers 75% of the rear surface, while the phosphorus BSF covers 25% of the rear surface. On the front, a 2-layer stack of thin thermal oxide and LPCVD silicon nitride is used to provide good surface passivation and anti-reflection properties. No texturing was used in this fabrication process. The innovative features of all-back-contact (ABC) cells developed at ANU involve uninterrupted p-n junctions with no gap in between them for simplified processing and a single-step diffusion enabling both light phosphorus diffusion at the front and heavy phosphorus diffusion at the rear. The cell process incorporating the above features has already led to solar cells with efficiency of over 19%, despite the small number of cells processed as yet.

INTRODUCTION

In June 2010, the leading PV manufacturer Trina Solar and SERIS started a 3-year research collaboration aiming at the development of all-back-contact (ABC) solar cells, using Trina's n-type monocrystalline Cz silicon wafers (125 mm wide, pseudo-square). The project aims to realise 21.5% on the production line for screen-printed ABC cells and 23.5% efficiency in the laboratory for full-size ABC cells with evaporated contacts [1]. One component of the 23.5% laboratory ABC cell development work is performed at ANU, where project researchers develop processing sequences for high-efficiency ABC cells with evaporated contacts, using small-sized solar cells (16 cm^2). The work at ANU started in February 2011.

All-back-contact cells were first proposed in 1975 by Schwartz and Lammert of Purdue University for concentrator applications [2,3]. Researches on ABC cells were further carried out by Sandia [4,5] and Stanford [6,7]. SunPower was established in 1985 to commercialise the Stanford developed technology and in 2010 reported efficiencies of large-area solar cells (155.1 cm^2) of up to 24.2% in a commercial production environment [8]. Primary advantages of ABC solar cells include: no metal shading on front surface; a higher metal coverage (since there is no trade-off between metal and shading); better surface passivation of sunward surface (since the front surface is not contacted and since lateral transfer of current is less important); improved rear optics and light trapping; simpler interconnecting system; and easy adoption of n-type Si, whose lifetime is less susceptible to metal and oxygen impurities. Despite the many advantages, ABC cells face the challenges of requiring high-lifetime Si, low front surface recombination, and fabrication complexity.

In this paper, we report on the progress with the development of 16-cm^2 ABC solar cells at ANU. The 19% efficient ABC cells, incorporating n^+ BSF and p^+ emitter at the rear and FSF with no texturing, represent a good interim result, considering the high optical losses due to the non-textured front surface. Further refinements of this process (for example inclusion of a textured front surface, decreasing the pitch, and

increasing the metal coverage on the rear) are expected to lead to significant efficiency improvements in the coming months. In this publication we describe the solar cell structure, fabrication sequence, current-voltage performance and characterisations.

CELL STRUCTURE

The cell structure adopts a simple approach with a planar surface at the sunward side. The front surface is diffused lightly with phosphorus. At the rear surface, n^+ BSF and p^+ emitter are formed in an interdigitated format which leaves no gap between opposite diffusions (n^+ and p^+), to minimise the fabrication complexity. A thermally grown thin silicon oxide and LPCVD SiN_x stack is formed on both wafer surfaces, to provide surface passivation and reflection reduction (on the front surface). Vacuum evaporated Al ($\sim 1.5 \mu\text{m}$) makes contact to the BSF and emitter regions via point contacts through the rear oxide/nitride stack, to maximise the rear surface passivation. Figure 1 shows the schematic structure of the resulting ABC solar cell.

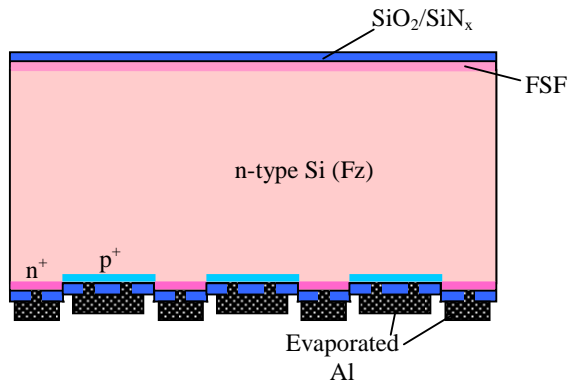


Figure 1: Schematic structure of 19% efficient ABC cells.

FABRICATION OF CELLS

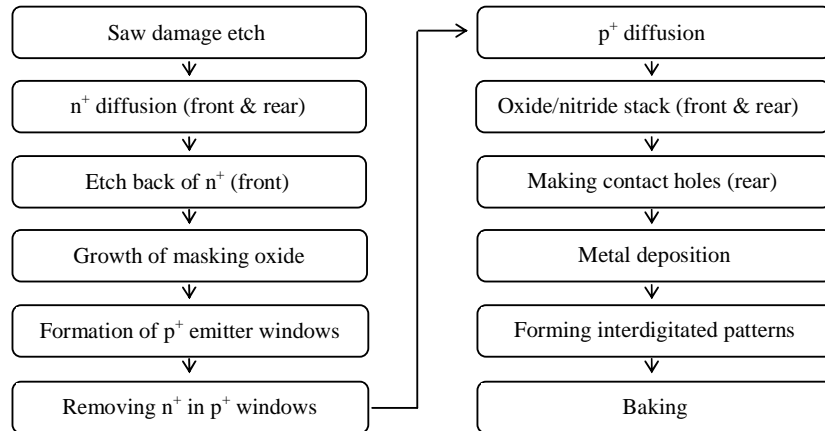


Figure 2: The process flow of the fabricated ABC silicon wafer solar cells.

The starting material of the cells are $\sim 1 \Omega\text{cm}$ 300 micron thick $\langle 100 \rangle$ n-type float-zone wafers. First, the wafers are saw damage etched and thinned down to 250 microns. A heavy phosphorus diffusion (n^+) is processed on both front and rear of the wafers, followed by in-situ oxide growth. Single-sided oxide etching is then carried out on the wafer, and the exposed n^+ diffusion is then etched back in tetramethylammonium hydroxide (TMAH) to give a light phosphorus diffusion (FSF), while leaving the rear n^+ untouched – thus enabling a cell with FSF and n^+ at the rear. Next, a thick masking oxide is grown on both sides and windows for the p^+ emitters at the rear surface are formed by lithographic means. The n^+ diffusion in the emitter

regions is then removed in TMAH at 85 °C for 2-3 minutes, followed by the p⁺ emitter diffusion. The masking oxide is then removed, and a stack of oxide and nitride is grown on both surfaces for passivation and anti-reflection purposes. The sheet resistance of FSF and n⁺ following all thermal process steps are ~160 Ω/□ and 15 Ω/□ respectively. Thousands of contact holes – 5 micron diameter holes with 70 micron pitch – are then formed by lithography at the rear surface. Following the opening of contacts, metal (~1.5 μm Al) is evaporated in vacuum environment to cover the entire rear surface. A photo-mask was then used to transfer interdigitated patterns on the rear surface by lithography means, leaving the metal in between p⁺ and n⁺ unprotected by the photoresist. The exposed metal is then etched off to form interdigitated patterns. The cells are then baked and diced out of the host wafer.

PERFORMANCE OF CELLS

The 16-cm² cells were measured under the AM1.5G spectrum from a flash tester [9]. Figure 3 shows the I-V performance of four ABC cells and Table 1 summarises the electrical parameters. All cells have open-circuit voltages of at least 680 mV, which demonstrates that the cells have very good surface passivation due to the oxide. The high short-circuit current densities of these planar cells also show that the high bulk lifetime of the starting wafers has been maintained. Fill factors (FF) exceeding 79% confirm that the total series resistance is relatively small for n⁺ and p⁺ finger designs based on 25% and 75% of the rear surface.

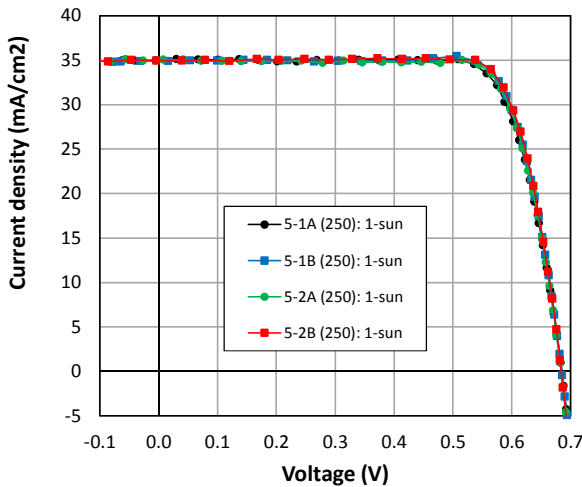


Figure 3: Measured one-sun I-V curves of four 16-cm² ABC solar cells made at ANU.

Table 1: Measured one-sun parameters of the four solar cells of Fig. 3.

ID	V _{oc} (V)	J _{sc} (mA/cm ²)	FF	Eff (%)	R _{sh} dark (Ω-cm ²)	R _s dark (Ω-cm ²)	R _s light (Ω-cm ²)	J01 (fA/cm ²)
5-1A (250)	683.2	35.0	0.782	18.7	7.3E+03	0.25	1.3	100
5-1B (250)	681.4	34.9	0.804	19.1	1.0E+05	0.25	0.9	110
5-2A (250)	682.5	34.9	0.794	18.9	2.1E+03	0.25	1.1	105
5-2B (250)	682.0	35.0	0.805	19.2	3.3E+05	0.25	0.8	105

CELL CHARACTERISATION

Photoconductance decay (PCD)

PCD measurements [10], which allow the extraction of the minority carrier lifetime, were used to identify the potential device performance. These measurements were performed after the final high-temperature processing step (i.e., prior to metallisation). As shown in Fig. 4, the high effective carrier lifetimes (~700 μs at an injection level of 1×10¹⁵ cm⁻³) at this stage indicate that good surface passivation is maintained up to the metallisation step. Furthermore, the measured high bulk lifetimes (determined using hydrofluoric acid assisted surface passivation) also confirm the high quality of the ANU processing sequence.

Shunt Resistance (R_{sh})

The shunt resistance of each cell was determined from the dark I-V curve at small forward-bias voltages (see Fig. 5). An excellent shunt resistance (100-200 $k\Omega\text{cm}^2$) was achieved for all cells fabricated. This is remarkable, since ABC cells with overlapping n^+ and p^+ diffusions are prone to shunting [11].

Reflection & QE

The optical characterisation was undertaken by measuring the front surface reflectance of the cells (see Fig. 6). The oxide/nitride stack provides good passivation via the oxide, while the oxide (~20 nm) is thin enough to not interfere significantly with the anti-reflection properties of the silicon nitride layer. Based on the measured reflectance data, external quantum efficiency (EQE) was modelled by the ratio of J_{sc} collected (equation 2) to the J_{sc} available (equation 1). In equation (1) it is assumed that every photon incident onto the solar cell is absorbed and collected by the solar cell device whose band gap best matches the photon energy. In the equation (1) and (2) $\Phi(\lambda)$ is the spectral irradiance of the incident solar spectrum, q is charge density, λ is wavelength, s is shading loss, C is collection efficiency, $r(\lambda)$ is the reflection as a function of wavelength, $\alpha(\lambda)$ is the absorption coefficient as a function of wavelength, W is the solar cell thickness, h and c are constants. The modelled J_{sc} and measured J_{sc} are quite comparable. The modelled EQE curve peaks at 96%.

$$J_{sc-avail} = q \int_{\lambda}^{\lambda_1} \frac{\phi(\lambda)}{hc/\lambda} d\lambda \quad (1)$$

$$J_{sc-col} = q(1-s)(1-C) \int_{\lambda}^{\lambda_1} (1-r(\lambda)) \frac{\phi(\lambda)}{hc/\lambda} (1-e^{-\alpha(\lambda)W}) d\lambda \quad (2).$$

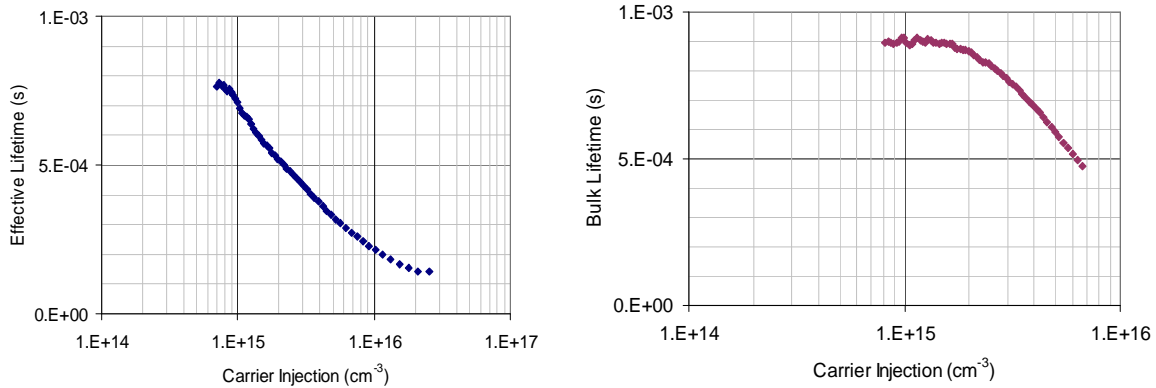


Figure 4: Effective carrier lifetime (left) and bulk lifetime (right) of a sample after the final high-T process.

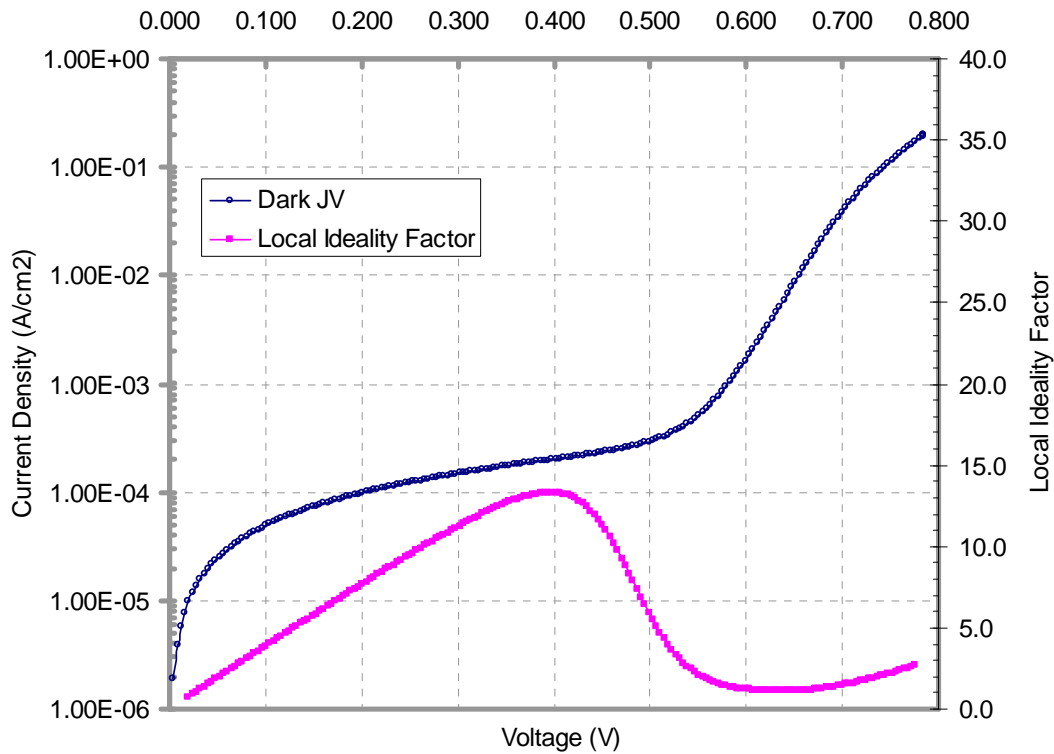


Figure 5: Dark I-V curve of one of the fabricated ABC cells.

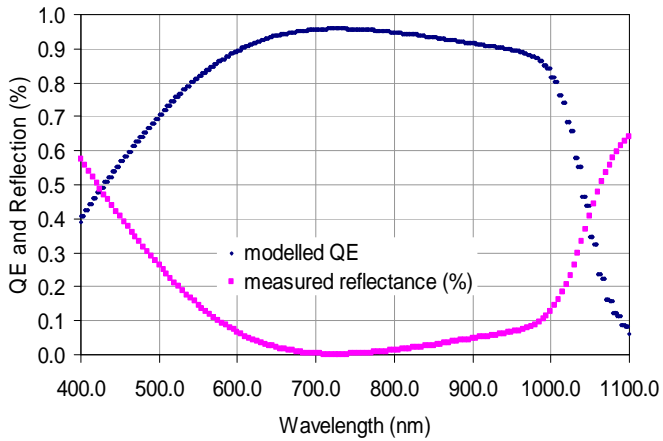


Figure 6: Measured reflectance of the ABC cell (lower curve) and modelled EQE (upper curve).

Suns- V_{oc}

$Suns-V_{oc}$ measurements were performed on ABC cells under high illumination intensities (0.6-30 suns). Such measurements are well suited for detecting contacting issues in the cells. The ABC cells developed at ANU exhibit a linear increase of voltage with illumination intensity (see Fig. 7). This demonstrates that the contacts are well behaved (i.e., ohmic).

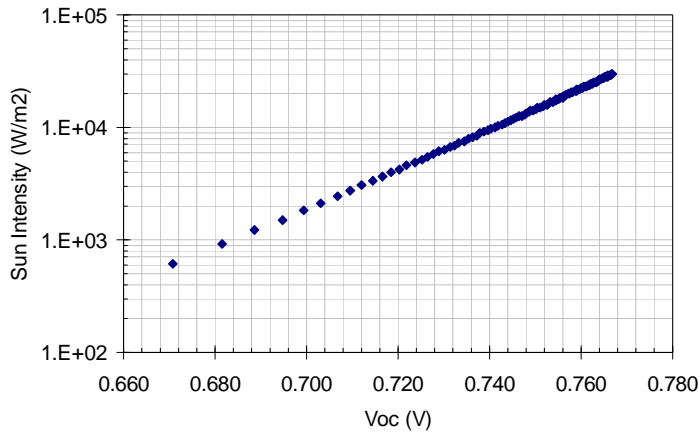


Figure 7: Suns- V_{oc} measurement of an ABC cell.

Baking

The behaviour of cell performance was also analysed by baking the cells at different temperatures in a forming gas environment. The investigated temperature range is from 250 °C to 350 °C. As shown in Fig. 8, the performance of the cells did not change significantly up till 300 °C baking, but at 350 °C the cell performance degraded drastically due to major reductions in V_{oc} , FF and J_{sc} . The degradation is believed to be due to aluminium spiking into the diffused regions, shunting the p-n junctions. For these 19% efficient ABC cells, baking in forming gas up to 300 °C is found to be optimal.

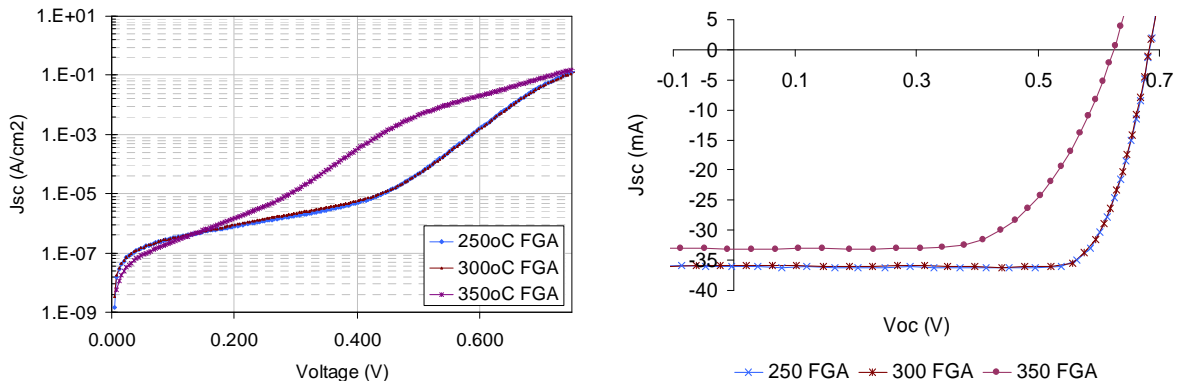


Figure 8: Performance of ABC cells after baking at different temperatures.

CONCLUSIONS

The 16-cm² cells incorporating a light phosphorus diffusion at the front, n⁺ BSF and p⁺ emitter at the rear, a stack of thin oxide and ARC nitride, fabricated from planar n-type FZ wafers at ANU have achieved an average conversion efficiency of 19.0%. The high bulk lifetime of the starting wafers is maintained after the final high-temperature processing step. Although the ABC cells developed at ANU have overlapping n⁺ and p⁺ diffusions, the shunt resistance of the cells is excellent. The J_{sc} modelled from the measured reflectance data indicates that the cells have an EQE of above 90% for a wide wavelength range. Inclusion of optimised diffusions at the electrical contacts ensures that no non-ohmic contact behaviour is present in these ABC cells. Baking the finished cells for 30 minutes in forming gas at a temperature in the 250-300 °C range improves the cell efficiency and does not yet cause shunting of the p-n junctions due to metal spiking. Besides, the successful demonstrations of the single-step diffusion, assisted by etching back the front, enabling light phosphorus diffusion at the front and heavy phosphorus diffusion at the rear; and the

simplified processing technique of forming uninterrupted interdigitated p and n diffusions at the rear, while avoiding the potential low shunt resistance confirm that the ABC cell fabrication techniques developed at ANU align with the industry's objective of manufacturing solar cells in a cost-effective way. Cell efficiencies higher than 19% are achievable with further refinements of the process, such as texturing, smaller pitch, increasing metal coverage and advanced passivation techniques.

Acknowledgements

Funding of this work by Trina Solar is acknowledged. The Solar Energy Research Institute of Singapore (SERIS) is sponsored by the National University of Singapore and Singapore's National Research Foundation through the Singapore Economic Development Board.

References:

1. Limited, T.S. <http://phx.corporate-ir.net/phoenix.zhtml?c=206405&p=irol-news&nyo=1>. June 2010.
2. Schwartz, R.J. and M.D. Lammert, *Silicon solar cells for high concentration applications*, in *Proc. IEEE International Electron Devices Meeting*, 1975, Washington DC.
3. Lammert, M.D. and R.J. Schwartz, *The interdigitated back contact solar cell: a silicon solar cell for use in concentrated sunlight*. IEEE Trans. Electron Dev. 1977, **24**: p. 337-342.
4. Garner, C.M., R.D. Nasby, and F.W. Sexton, *An interdigitated back contact solar cell with high-current collection*. IEEE Electron Dev. Lett. 1980, **1**: p. 256-258.
5. Garner, C.M., et al. *An interdigitated back contact solar cell with high-current collection*. in *Proc. 15th IEEE PVSC*, 1980, Orlando.
6. Swanson, R.M. *Point-contact solar cells: theory and modelling*. in *Proc. 18th IEEE PVSC*, 1985, Las Vegas.
7. Swanson, R.M., et al., *Point-contact silicon solar cells*. IEEE Trans. Electron Dev., 1984, **31**: p. 661-664.
8. Cousins, P.J., et al. *Generation 3: Improved performance at lower cost*. in *Proc. IEEE PVSC*, 2010, San Diego.
9. Keogh, W.M., A. Blakers, and A. Cuevas, *Constant voltage I-V curve flash tester for solar cells*. Solar Energy Materials and Solar Cells, 2004, **81**: p. 183-196.
10. Sinton, R.A. and A. Cuevas, *Contactless determination of current-voltage characteristics and minority-carrier lifetimes in semiconductors from quasi-steady-state photoconductance data*. Applied Physics Letters, 1996, **69**: p. 2510-2512.
11. Guo, J.-H. and J.E. Cotter. *Interdigitated Backside Buried Contact Solar Cells*. in *Proc. 3rd World Conference on Photovoltaic Energy Conversion*, 2003, Osaka, Japan.